

Graphite multilayer thin films: a new anode material for Li-ion microbatteries synthesis and characterization

M. Hess, E. Lebraud, A. Levasseur *

Institut de Chimie de la Matière Condensée de Bordeaux (ICMCB), Ecole Nationale Supérieure de Chimie et Physique de Bordeaux (ENSCP), avenue Pey Berland, BP 108, 33402 Talence Cedex, France

Accepted 24 September 1996

Abstract

A thin-film carbon anode was prepared by a repeat deposition process from a commercial graphite dispersion, Archeson Aquadag[®], which produced non-turbostratic films. Electronic conductivity measured with an aligned four-point set-up is lower than that of pure graphite. Cyclic voltammetry studies show that these thin films present the usual intercalation stages of lithium in graphite. © 1997 Published by Elsevier Science S.A.

Keywords. Lithium-ion batteries; Graphite; Thin films; Anode materials

1. Introduction

Carbon anodes store energy by forming a lithium–graphite intercalation compound (Li–GIC), Li_xC_6 ($0 < x \leq 1$) [1–5]. The attainable values of x for reversible intercalation are determined by the purity and crystallinity of the carbon, the nature of the electrolyte [6,7] and the experimental conditions used [8]. Graphitic carbon materials intercalate electrochemically Li ions from suitable electrolytes [9,10] up to a value of $x \approx 1$ and show a marked staging phenomenon [11,12] whereas, in more disordered, turbostratic [13] or in completely amorphous carbons, the staging is suppressed [14] and x remains below 0.7.

In previous work [15] we reported that a thin-film carbon anode can be fabricated by a deposition process from a commercial graphite dispersion. Graphite multilayer thin films (GMTF) prepared by repeated substrate induced coagulation were identified as a thoroughly porous network of agglomerated well-crystallized graphite particles. Despite the apparent disorder of smaller particles, however, it is noted that larger particles are preferentially aligned, parallel to the substrate surface, forming a lamellar substructure (Fig. 1). We believe that this phenomenon is due principally to the

multilayer deposition process. The film thickness determined by scanning electron microscopy (SEM), revealed that a typical ten-layer deposit has a thickness of approximately 800 nm.

The intercalation behaviour of graphite is particularly influenced by electrolyte–surface interactions [16,17], which cause surface-bound passivation layers protecting the bulk of the electrode from further electrolyte attack. Porous thin films, whose bulk is negligible compared with its surface encounter a more severe attack than thick and compact electrodes. Hence, we are hesitating about the application of GMTFs in liquid electrolytes. Application of this material in more sophisticated battery set-ups, e.g. in inorganic solid-state microbatteries, however, seems to be appropriate.

In this work, cyclic voltammetry and conductivity studies on GMTFs are presented. Monitoring the electronic conductivity is a fundamental step in the development of thin-film devices for two important reasons: first, thin-film configurations use frequently materials whose electronic bulk conductivity is poor, but they possess other material properties being profitable to their application. Second, the electronic conductivity measurements provide a non-invasive analysis method, which is very sensitive to surface contamination, in particular to that occurring in deposits from multicomponent solutions.

GMTFs should facilitate electrochemical intercalation because of the presence of many grain boundaries, pores and

* Corresponding author.



Fig. 1. SEM graph (10 kV, $\times 40000$) of a 10 GMTF, cross section on a glass slide

partly disordered particle distribution. As the basic material is graphite, the typical staging phenomenon during electrochemical Li intercalation should be observed. Reversible (de-)intercalation as well as irreversible solvent co-intercalation can be easily demonstrated using slow-scan cyclic voltammetry.

2. Experimental

The detailed fabrication process of GMTFs has been presented in Ref. [15]. For convenience, each GMTF was named after the number of deposits, for instance 10 GMTF represents a ten-layer GMTF. GMTFs deposited on glass slides were

used to determine the electronic conductivity as a function of temperature. Subsequent to the deposition process, all samples were made and passed through a hot fan drying step and stored for a few days in an argon-filled glove box. Due to their conductivity behaviour we consider these as wet samples, whereas dried GMTFs are prepared easily by heating at 270°C under vacuum for at least 48 h. Temperature scans were carried out under dynamic vacuum in a home-made temperature-controlled Dewar cell, which was assembled for each measurement in an atmosphere-controlled argon glove box. Laplume's [18] aligned four-point set-up and his approximation of the three-dimensional potential distribution in thin films were used to obtain the conductivity of GMTFs.

The cyclic voltammetry experiments were performed in a closed button cell-type configuration, in which a stainless-steel disc supported GMTF and a bulk lithium counter electrode were superposed. This sandwich was separated by electrolyte supplying Whatman GF/C glassfiber layers (Whatman International, Maidstone, UK). 1 M LiClO_4 in propylene carbonate (PC)/ethylene carbonate (EC) (50/50 by volume) was used as the electrolyte. The salt was dried under secondary vacuum. PC as well as EC were distilled under vacuum. The voltammograms at 0.01 mV/s were recorded by an EG&G PAR potentiostat/galvanostat Model 273 against an Li/Li^+ reference electrode. All electrochemical measurements were undertaken in a purified argon atmosphere.

3. Results and discussion

The fabrication process of GMTFs involves a variety of different reactants such as water, surfactants, gelatine and electrolytes. These compounds should be considered as pos-

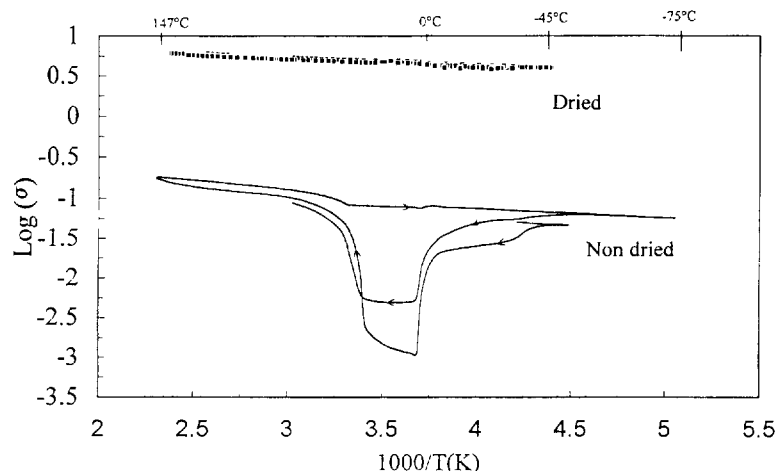


Fig. 2. Logarithm of electronic conductivity vs. inverse temperature for a 10 GMTF.

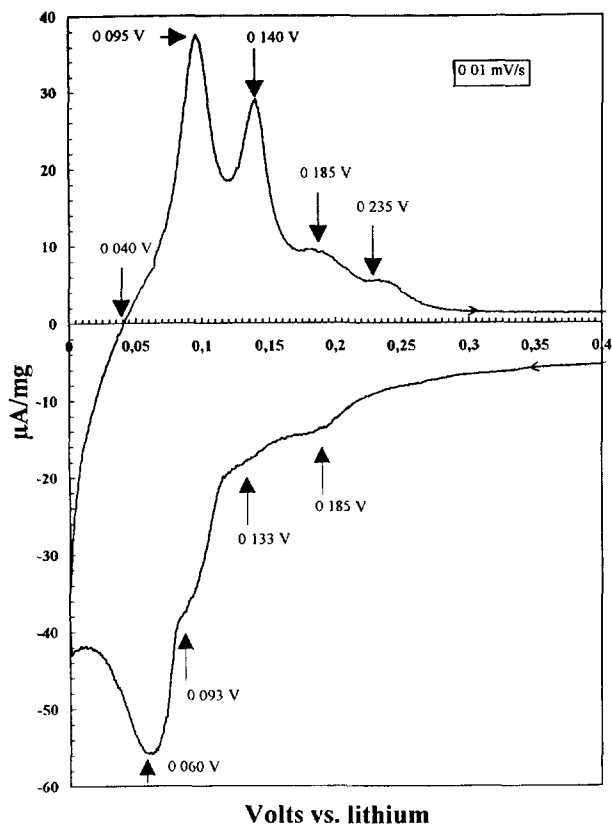


Fig. 3. First voltammetric cycle (0.01 mV s^{-1}) of a 10 GMTF.

sible contamination, which inevitably will influence the conductivity behaviour. In Fig. 2, the electronic conductivities taken during a temperature cycle of a dried 10 GMTF are shown. The curve illustrates a metal-like conductivity behaviour without any incongruities. Water contamination can be traced immediately by the appearance of a broad irreversible peak between -4 and 25°C . The room temperature (25°C) resistivity ($\rho_{25} = 3.3 \times 10^{-2} \Omega \text{ m}$) is considerably higher compared with that of bulk graphite ($\rho_{25} = 4.0 \times 10^{-3} \Omega \text{ m}$) (intraplane [19]). This is due to the inhomogeneous nature of the thin film, whose overall resistivity is governed by the grain boundary interconnection resistances. As the interplane resistivity ($\rho_{25} = 0.6 \Omega \text{ m}$) is about four decades higher than that of the intraplane resistivity, it can be assumed that a considerable portion of the GMTFs' overall resistivity is caused by particles whose graphitic planes are perpendicularly orientated towards the current lines. In fact, the observed room temperature conductivity of $\sigma_{25} = 3.02 \text{ cm}^{-1}$ is sufficient for application in thin-film set-ups.

The first voltammetric cycle (0.01 mV s^{-1}) of 10 GMTF is illustrated in Fig. 3 ($0 \text{ V} \leq U \leq 0.4 \text{ V}$).

During the reduction process the cathodic current appeared from approximately 1.2 to 0.0 V . Besides a slightly elevated value of the current we did not observe any irreversible cathodic solvent co-intercalation peak between 0.5 and 1 V

[20,21]. Lithium intercalation starts at about 0.25 V and is represented by a very broad but structured reduction peak. Three distinct shoulders are visible at 0.185 , 0.133 and 0.093 V . The first one corresponds to the transition between a slightly randomly intercalation state to stage 4. The second and third shoulders correspond to the transition from stages 4 to 3 and 3 to 2, respectively. The main peak at 0.06 V corresponds to the transition from stage 2 to 1 resulting in the formation of LiC_6 . During the oxidation process two peaks and two shoulders can be seen corresponding to the de-intercalation of lithium stage by stage. This voltammetric cycle represents, perhaps the clearest demonstration of the intercalation stages of lithium in graphite [22,23].

The results obtained from analysis of mesocarbon microbeads (MCMB) by Mabuchi et al. [24] confirm this assignment; these authors found a good agreement between the peak assignments of their cyclic voltammogram and the identification of the stage by X-ray diffractometry.

4. Conclusions

Graphite multilayer thin films present a metal-like conductivity and a resistivity higher than bulk graphite. The cyclic voltammetry study shows that these thin films exhibit a typical pure graphite behaviour. The use of these thin films as a negative electrode in microbatteries is in progress.

References

- [1] D. Guerard and A. Herold, *Carbon*, 13 (1975) 337.
- [2] T. Ohzuku, Y. Iwakoshi and K. Sawai, *J. Electrochem. Soc.*, 140 (1993) 2490.
- [3] K. Sawai, T. Ohzuku and T. Hirai, *Chem. Express*, 5 (1990) 837.
- [4] J.R. Dahn, *Phys. Rev. B*, 44 (1991) 9179.
- [5] R. Yazami and D. Guerard, *Ext. Abstr., Meet The Electrochemical Society, Proc. Vol. 92-2, Toronto, Ont., Canada, 11–16 Oct. 1992*, Abstr. No. 24, p. 32.
- [6] I. Kuribayashi, M. Yokoyama and M. Yamashita, *J. Power Sources*, 54 (1995) 1.
- [7] A. Ohta, H. Koshina, H. Okuno and H. Murai, *J. Power Sources*, 54 (1995) 6.
- [8] J.R. Dahn, A.K. Sleight, H. Shi, J.N. Reimers, Q. Zhong and B.M. Way, *Electrochim. Acta*, 38 (1993) 1179.
- [9] Z.X. Shu, R.S. McMillan and J.J. Murray, *Proc. Symp. New Sealed Rechargeable Batteries en Supercapacitors, 1993*, The Electrochemical Society, Proc. Vol. 93-22, 1993, p. 238.
- [10] D. Guyomard and J.M. Tarascon, *J. Power Sources*, 54 (1995) 92.
- [11] Z.X. Shu, R.S. McMillan and J.J. Murray, *J. Electrochem. Soc.*, 140 (1993) 922.
- [12] D. Billaud, F.X. Henry and P. Willmann, *Mater. Res. Bull.*, 28 (1993) 477.
- [13] P. Schoderbock and H.P. Boehm, *Mater. Sci. Forum*, 91–93 (1992) 683.
- [14] J.R. Dahn, R. Fong and M.J. Spoon, *Phys. Rev. B*, 42 (1990) 6424.

- [15] M. Hess, E. Lebraud, A. Levasseur and M. Chambon, *Thin Solid Films*, in press.
- [16] D. Aurbach, Y. Ein-Eli, O. Chusid (Youngman), Y. Carmeli, M. Babai and H. Yamin, *J. Electrochem. Soc.*, *141* (1994) 603.
- [17] J.O. Besenhard, M.W. Wagner, M. Winter, A.D. Jannakoudakis, P.D. Jannakoudakis and E. Theodoridou, *J. Power Sources*, *43–44* (1993) 413.
- [18] J. Laplume, *Rev. Soc. Radioélectriciens Paris*, *35* (335) (1955) 113
- [19] E.L. Piper, *Soc. Min. Eng. AIME, Repr. No. 73-H-14* (1973).
- [20] J.O. Besenhard, M. Winter, J. Yang and W. Biberacher, *J. Power Sources*, *54* (1995) 228.
- [21] J.O. Besenhard and H.P. Fritz, *J. Electroanal. Chem.*, *53* (1974) 329.
- [22] T. Zheng, J.N. Reimers and J.R. Dahn, *Phys. Rev. B*, *51* (1995) 734.
- [23] M.W. Verbrugge and B.J. Koch, *J. Electrochem. Soc.*, *143* (1996) 24.
- [24] A. Mabuchi, H. Fujimoto, K. Tokumitsu and T. Kasuh, *J. Electrochem. Soc.*, *142* (1995) 3049.